Observation of antiferromagnetic coupling in epitaxial ferrite films

I. Knittel,[1] J. Wei,[1] Y. Zhou,[2] S. K. Arora,[2] I. V. Shvets,[2] M. Luysberg,[3] and U. Hartmann[1]
[1]*Department of Experimental Physics, University of Saarbrücken, Saarbrücken, Germany*
[2]*SFI Nanoscience Laboratory, School of Physics, Trinity College, Dublin 2, Ireland*
[3]*Ernst-Ruska-Zentrum, Jülich Research Center, Jülich, Germany*
(Received 4 September 2006; published 19 October 2006)

Defects in ferrite can change the local magnetic coupling from ferromagnetic to strongly antiferromagnetic. In eptiaxial magnetite (Fe_3O_4) films, defects locally altering exchange interaction, i.e., "antiphase boundaries" (APB), essentially determine magnetic and magnetotransport properties. We locally observed specific magnetization reversal events in epitaxial magnetite $Fe_{3-\delta}O_4$/MgO films ($\delta \approx 0.03$) by magnetic force microscopy in external magnetic fields. A dominating phenomenon is pinning of bubble domains at single APB. Pinning is a particular consequence of antiferromagnetic coupling across APB. Antiferromagnetic coupling across APB could be directly verified for a sample with an APB domain size above the resolution limit of magnetic force microscopy.

DOI: 10.1103/PhysRevB.74.132406 PACS number(s): 75.70.Kw, 75.50.Gg, 75.70.Ak

Ferrites contain two magnetic sublattices which are coupled by antiferromagnetic superexchange. A net magnetization results because the magnetic moments of the sublattices are unequal. Certain defects within a ferrite can change the local exchange constant from a ferromagnetic to an antiferromagnetic (AF) one.[1] In this study, defects denoted as "antiphase boundaries" (APB) in epitaxial ferrite films are of particular importance. APB arise when the rotational symmetry of the substrate is higher than that of the ferrite film or when the lattice constant of the film is an integer multiple of that of the substrate. If, during growth of the magnetic film, islands merge, defects can be formed at the boundaries between those islands that are mutually rotated or translated by a fraction of the unit cell.[1,2] In Fig. 1 the example of an APB in magnetite is shown schematically in detail. Fe_3O_4 (001) grown on MgO (001) is considered. Here, coupling across most APB is of the AF type. Cumulative effects of AF defects in ferrite materials are usually treated in terms of an inhomogenous exchange interaction. They are a source of domain-wall pinning.[1,2] In several epitaxial ferrite film arrangements, mainly prepared for microwave applications, the contribution of APB to the magnetic behavior has been quantified.[1] Fairly recently, it was found that the magnetic properties of Fe_3O_4 are clearly dominated by APB with AF coupling.[1] Because of its high spin polarization,[3] conductivity, and high Curie temperature, Fe_3O_4 is a prime candidate material for spin electronics.[4] Much effort was spent to prepare epitaxial thin films, in particular on MgO. However, the magnetic domain structure and the overall magnetic properties have been found to be very different from the bulk.[5] Namely, high saturation fields, low saturation magnetization,[5] superparamagnetism of thinner films,[6] unexpected out-of plane moments,[7] and an irregular magnetic domain structure[8] have been observed. The key to these unusual properties of Fe_3O_4 thin films is the observation of a large density of APB by transmission electron microscopy (TEM),[8] and the analysis of the various types of APB.[9]

With respect to spin-electronics applications, the presence of APB is considered a major obstacle. Recently, however, it was shown that the "domain-wall resistance" across an APB is huge.[10] This implies that it could be possible to use the APB itself as a spin valve.[10] A first step toward this direction is the growth of APB in a controlled manner at atomic steps of the substrate.[11]

Increasing the "antiphase domain size," i.e., the average distance between APB, is a key challenge for achieving epitaxial films resembling bulk Fe_3O_4 properties. Antiphase domain sizes of about 50 nm can be achieved by annealing.[12] The magnetic structures in the presence of APB found so far are irregular.[7,13]

In this study we employed epitaxial Fe_3O_4 films that were subjected to a short mild annealing under ambient conditions (250 °C, 4 min). Such a post-growth annealing only marginally changes the stochiometry of magnetite to $Fe_{3-\delta}O_4$ with a value of $\delta \approx 0.03 \pm 0.01$ as determined from Mössbauer measurements.[15] The rather high stochiometric resolution was obtained by a sufficiently long averaging period. There are no second-phase inclusions formed in the film as a result of the annealing procedure. The films exhibit an enhanced

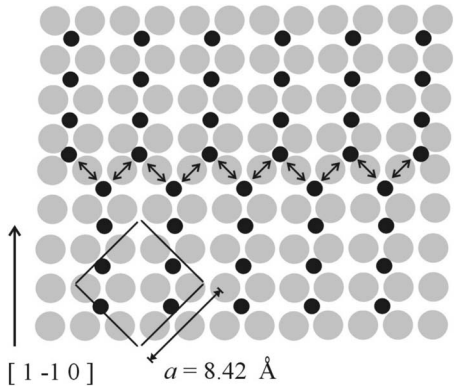

FIG. 1. Schematics showing a Fe_3O_4(100) layer grown on MgO(001). Oxygen ions are displayed in grey, *B*-site iron ions, which form the sublattice dominating magnetization, are displayed in black. An antiphase boundary (APB) formed by a shift of the upper part by $a/(2\sqrt{2})$ along [1–10] is shown. This shift is equivalent to a rotation by 90° with simultaneous translation by $a/2$ along [001]. Across the APB there are additional 90°—Fe-O-Fe bonds (arrows). Such links exhibit strong AF coupling by superexchange.

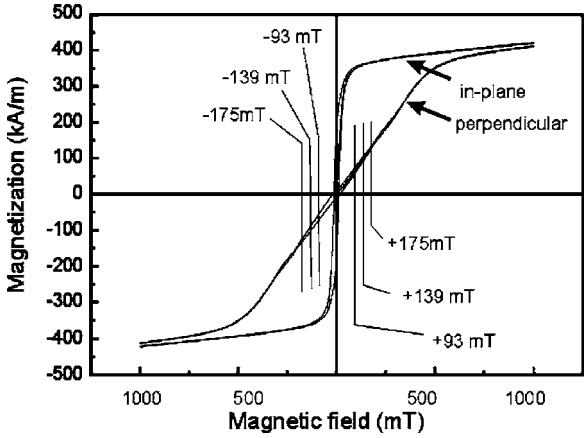

FIG. 2. Magnetization hysteresis curves of a magnetite film employed for the study, and the values of the perpendicular magnetic field used for MFM. After applying a negative field, the remanent, and the positive field MFM images were recorded, then the images for negative values of increasing amplitude.

saturation magnetization after annealing.[14] An enhanced saturation magnetization indicates a lower density of magnetically active APB as compared to stochiometrically pure Fe_3O_4.[14,15] In contrast to previous observations, magnetic force microscopy (MFM) reveals a regular magnetic domain structure.[15] The domain pattern has been identified as "weak stripe domains."[16] It is strongly influenced by pinning.[15] Pinning centers are related to APB. We utilized the regular domain structure and the low APB density to image magnetization reversal and magnetic domains related to single APB.

A film of $Fe_{3-\delta}O_4/MgO$ (100) with $\delta \approx 0.03$ exhibiting a magnetic stripe-domain pattern was imaged by MFM at particular field strengths as indicated in Fig. 2. The resulting image sequence is shown in Fig. 3. In the remanent state, a

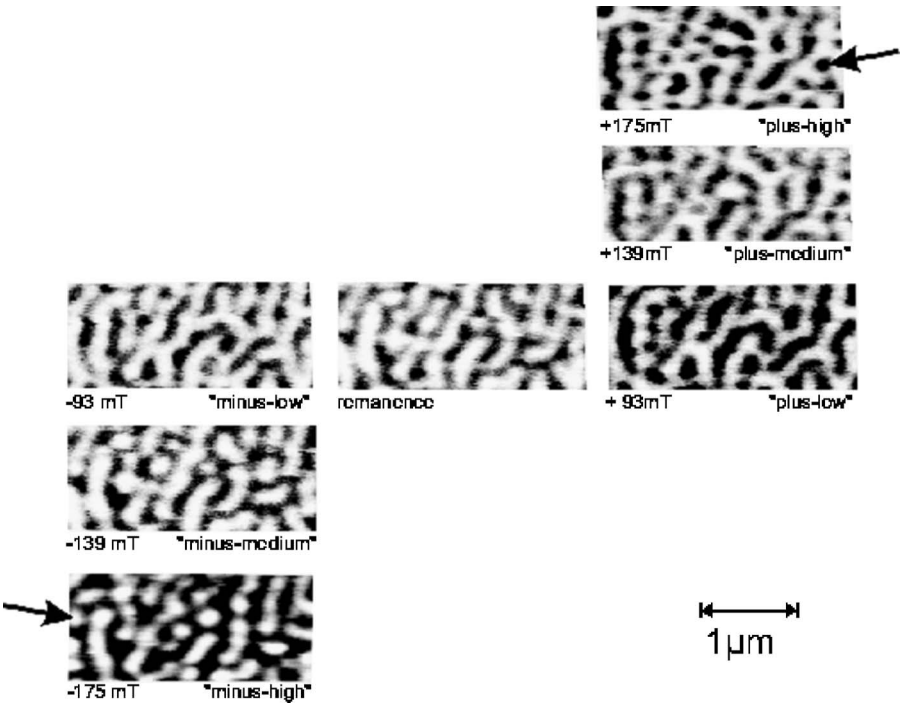

FIG. 3. MFM images of a representative film area during sweeping of the perpendicular field. For positive field values, images were inverted to account for the tip magnetization reversal. Arrows point to a typical dot. Because for every line, the average brightness is subtracted, the overall change in the magnetization is not reflected in the images.

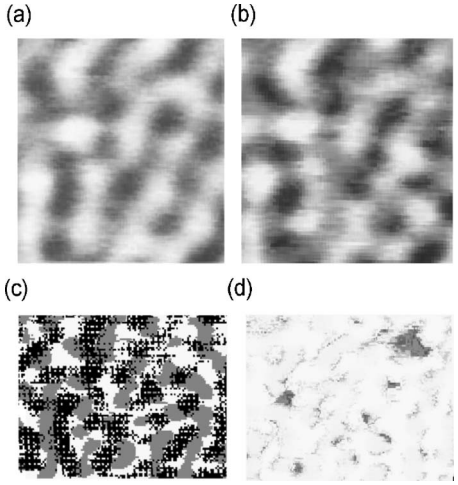

FIG. 4. (a) Superposition of all images from minus-medium to plus-medium. (b) superposition of the plus-high-field image and the minus-high-field image. (c) black dots in the plus-high-field image are displayed further in black, the white dots in the minus-high-field image are displayed in gray. (d) dark areas indicate changes from black in the plus-high-field image to white in the minus-high-field image.

stripe-domain structure is observed. In an external field perpendicular to the film, the stripe-domain structure partly decomposes into "dots" with polarizations oppositely to the external field, and also oppositely to the magnetization of the environment (arrows in Fig. 3). Between subsequent field steps, most of the magnetic pattern remains unchanged and therefore can be used for precise alignment of the images. In Fig. 4(a) images for field values from minus medium to plus medium were superimposed and averaged for some smaller area. In Fig. 4(b), the minus-high-field image is superimposed to the plus-high-field image. The structure is largely

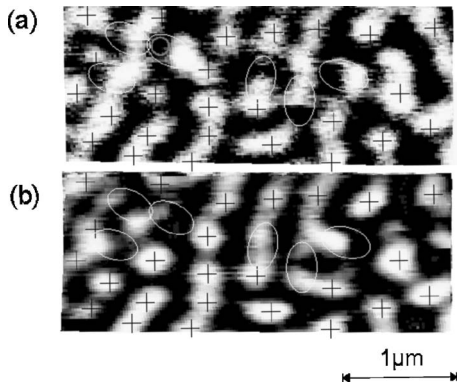

FIG. 5. MFM images of magnetite at (a) minus medium, (b) minus-high fields. Six locations of interest are shown by ovals. These include pairs of domains changing the contrast simultaneously: the black areas within each oval changes to white and vice versa. The magnetization of the environment (referenced by crosses) remains largely unchanged.

the same in both images. This confirms the immobility of the dots: A dot may change in size or polarization, but it does not move. In Fig. 4(c), the black dots of the plus-high-field image (displayed in black) are superimposed to the white dots of the minus-high-field image (displayed in grey). The pattern is clearly nonrandom, with a tendency of black dots to have white neighbors and vice versa. Black and white dots frequently appear in pairs. In Fig. 4(d), an AND operation was applied to the plus-high-field and the inverted minus-high-field image such that those areas are shown in dark, where the magnetization has changed from black in the plus-high-field to white in the minus-high-field image. This indicates that reversal of dots is rare. Most reversal events take place upon changing from minus-medium to minus-high field. In Figs. 5(a) and 5(b) most dots (indicated by crosses) remain unchanged by the change of the external field. A typical reversal event leads to a simultaneous change of contrast for a pair of domains. Six such pairs are marked by ovals in Figs. 5(a) and 5(b). They change contrast as the field increases from minus -medium to minus-high. In the following, we denote such pairs of domains as "dipolar centers." We believe that the observed dipolar reversal events are not induced by tip-sample interaction because we found them oriented in all directions relative to the scan. There is no correlation between the magnetic and the topography image for the MFM images published in this work. The magnetization-switching events were observed apart from the dominating background effect: Boundaries between black and white areas gradually move as the field sweeps and also the contrast between black and white neighboring areas changes. These observations at submicron scale correspond well with the overall magnetization curve (Fig. 2). The magnetization curve is essentially linear and nonhysteretic in the observed regime. This results from the incremental alignment of magnetization within the domains and mainly from the movement of the domain walls. Reversals of dipolar centers contribute to the small hysteresis observed.

The weak stripe domains investigated in this work can be compared[15] with similar patterns observed on strained

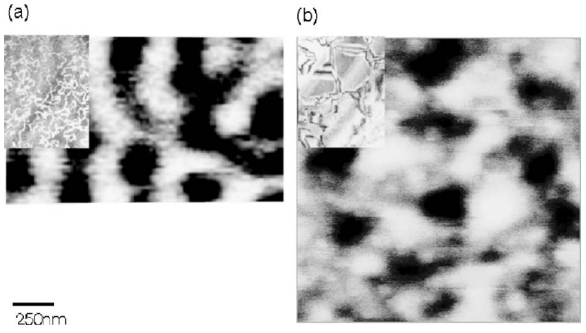

FIG. 6. MFM images (main images) of (a) the same film as in Figs. 1–5, with a thickness of 100 nm. (b) shows a similar film with thickness of 700 nm. Insets show TEM images of the APB structure (insets) for comparable films. All images are displayed at the same scale. The film in (b) has been thinned for TEM imaging.

permalloy,[16] cobalt,[17] and epitaxial iron (111) films.[18] In comparison to Ref. 17, the dots appearing at high field can be identified as magnetic "bubble domains." Bubble domains attach themselves to pinning sites.[18] That may explain the immobility of the dots, and their tendency to form dipolar centers in the plus-high-field and minus-high-field regimes (Fig. 4). Pinning of bubble domains is a well-known phenomenon. In contrast, magnetization reversal of dipolar centers, as shown in Fig. 5, is uncommon, and thus points toward an uncommon type of pinning site.

In the absence of pinning, a bubble domain of a certain volume V in its equilibrium position $x=0$ experiences to a first approximation a harmonic potential $E(x)$ generated by the environment. The exchange constant of the defect-free film is A_0 and the effective anisotropy is K. The domain-wall width is then given by $d \propto (A/K_{\mathrm{eff}})^{1/2}$. An interface within the film is assumed to have an effective exchange constant A_1. For a conventional planar pinning site one has $0 \leqslant A_1 < A_0$, while for a magnetically ineffective interface $A_1=0$. An interfac with AF exchange coupling has negative exchange constant A_1, where perfect coupling yields $A_1=-A_0$. The domain-wall energy is proportional to $|AK|^{1/2}$. Energy E_{wall} can be gained by a shift of the bubble by Δx, placing the domain wall right at the interface. The overall potential experienced by the bubble now is a double potential, with a threshold energy of $\Delta E_{\mathrm{wall}} \propto (A_0{}^{1/2} - |A_1|^{1/2}) K^{1/2}$. There will be a jump of the bubble to another equilibrium position, if there is an additional field gradient of $\partial H/dx$ to overcome the threshold energy. This process requires $\mu_0 |\partial H/\partial x| \Delta x M_s V > \Delta E_{\mathrm{wall}}$. The reversal events seen in Fig. 5 can be caused by AF interfaces with $A_1 < 0$, but also by conventional pinning, $0 < A_1 < A_0$. However, the pinning energy is higher for AF coupling: For an ideal AF interface it is twice that of a nonmagnetic interface. The reversal events in Fig. 5 do ultimately not allow us to distinguish the difference in pinning energies, because various parameters in the above model cannot be obtained with sufficient precision.

Figure 6 displays MFM images of two samples of different APB density. The APB have been revealed by transmission electron microscopy images shown as insets. In both cases (220) two beam imaging conditions were adjusted. As a result the APB in Fig. 6(a) shows bright contrast. In Fig.

6(b) APB are identified by the typical fringe contrast arising from phase shifts along inclined defects. For the film in Fig. 6(b) with a thickness of 700 nm the antiphase domain size is about 250 nm, in comparison to about 50 nm for the 200 nm thick film in Fig. 6(a). For the 100 nm thick films investigated with respect to their magnetic properties, an APB structure similar to that of Fig. 6(a) can be assumed.[10] The larger antiphase domain size of the thicker film is expected from Ref. 10. The antiphase domain size in Fig. 6(b) is well above the resolution limit of the MFM of about 80 nm in the present case. Figures 6(a) and 6(b) further show the magnetic domain structures of 100 nm and 700 nm thick films, respectively. In Fig. 6(b), the magnetic domain structure matches the antiphase domain structure. The magnetization tends to be oriented in opposite directions at APB, as expected for AF coupling. In contrast, in Fig. 6(a) the APB structure in the inset corresponds to the small-scale disorder present in the MFM image, while the magnetic domains are conventional stripe domains.

A priori, it can again not be excluded that nonmagnetic interfaces with $A=0$ are present with a respective structure. It is only in the high-field regime where the AF coupling leads to qualitatively new behavior. Above the nucleation field, a film with conventional pinning centers is saturated. At AF interfaces, a layer of opposite magnetization will persist, resulting in a reduced magnetization at high field. Since this is observed in all magnetization curves of the samples used in this study, there exists a high amount of AF coupling APB in the samples. It is therefore plausible that the results if Figs. 5 and 6 are at least in part caused by AF exchange coupling across APB.

Concerning future work, one should note that AF coupling across APB is not limited to ferrites, but also appears i.e., in the double perowskite Sr_2FeMoO_6.[19] Furthermore, high-resolution magnetic imaging of APB in magnetite has been performed recently by means of holography TEM.[20]

In conclusion, unique dipolar magnetic nanostructures were produced that are based on single antiphase boundaries, and antiparallel coupling across APB was imaged. We prepared magnetitelike $Fe_{3-\delta}O_4$, ($\delta \approx 0.03$) films on MgO (100). Such films provide a remanent stripe domain pattern, and bubble domains in an external magnetic field. Magnetic domain structures are strongly affected by pinning sites. In fields of ±175 mT, MFM images show an irregular array of dots of opposite magnetization. Dots appearing in opposite external fields are spatially correlated, with a tendency to form pairs. A few of such pairs show magnetization reversal during the field sweep. Reversal of dipolar centers was observed for isolated sites and in small groups. In a thick-film sample with a large APB size, MFM resolution is sufficient to directly resolve a magnetic domain structure mainly determined by APB. A tendency towards antiparallel magnetization across APB is observed.

The authors would like to thank Astrid Müller and Andreas Englisch, University of Saarbrücken, for the variable-field MFM setup. Patrick Steffen and Richard Pfeifer contributed to the MFM imaging. Thomas Sulzbach, Nanosensors GmbH, supplied the high-resolution MFM tips. This work is funded by the European Union within the ASPRINT project.

[1] Y. Suzuki, Annu. Rev. Mater. Res. **31**, 265 (2001).
[2] A. Lisfi and J. C. Lodder, J. Phys.: Condens. Matter **14**, 12339 (2002).
[3] W. E. Pickett and J. S. Moodera, Phys. Today **54** (5), 39 (2001).
[4] Y. S. Dedkov, U. Rüdiger, and G. Güntherodt, Phys. Rev. B **65**, 064417 (2002).
[5] D. T. Margulies, F. T. Parker, F. E. Spada, R. S. Goldman, J. Li, R. Sinclair, and A. E. Berkowitz, Phys. Rev. B **53**, 9175 (1996).
[6] F. C. Voogt, T. T. M. Palstra, L. Niesen, O. C. Rogojanu, M. A. James, and T. Hibma, Phys. Rev. B **57**, R8107 (1998).
[7] L. A. Kalev and L. Niesen, Phys. Rev. B **67**, 224403 (2003).
[8] D. T. Margulies, F. T. Parker, M. L. Rudee, F. E. Spada, J. N. Chapman, P. R. Aitchison, and A. E. Berkowitz, Phys. Rev. Lett. **79**, 5162 (1997).
[9] S. Celotto, W. Eerenstein, and T. Hibma, Eur. Phys. J. B **36**, 271 (2003).
[10] W. Eerenstein, T. T. M. Palstra, S. S. Saxena, and T. Hibma, Phys. Rev. Lett. **88**, 247204 (2002).
[11] S. K. Arora, R. G. S. Sofin, and I. V. Shvets, Phys. Rev. B **72**, 134404 (2005).
[12] W. Eerenstein, T. T. M. Palstra, T. Hibma, and S. Celotto, Phys. Rev. B **68**, 014428 (2003).
[13] J. F. Bobo, D. Basso, E. Snoeck, C. Gatel, D. Hrabovsky, J. L. Gauffier, L. Ressier, R. Mamy, S. Visnovsky, J. Hamrle, J. Teillet, and A. R. Fert, Eur. Phys. J. B **24**, 43 (2001).
[14] Y. Zhou, X. Jin, and I. V. Shvets, J. Appl. Phys. **95**, 7357 (2003).
[15] J. Wei, I. Knittel, Y. Zhou, F. T. Parker, I. J. Shvets, and U. Hartmann, Appl. Phys. Lett. (to be published).
[16] N. Saito, H. Fujiwara, and Y. Sugita, J. Phys. Soc. Jpn. **19**, 1116 (1964).
[17] M. Hehn, S. Padovani, K. Ounadjela, and J. P. Bucher, Phys. Rev. B **54**, 3428 (1996).
[18] S. Foss, C. Merton, R. Proksch, G. Skidmore, J. Schmidt, E. D. Dahlberg, T. Pokhil, and Y. T. Cheng, J. Magn. Magn. Mater. **190**, 61 (1998).
[19] J. Lindén, M. Karppinen, T. Shimada, Y. Yasukawa, and H. Yamauchi, Phys. Rev. B **68**, 174415 (2003).
[20] T. Kasama, R. E. Dunin-Borkowski, W. Eerenstein, Phys. Rev. B **73**, 104432 (2006).